Impact of the temperature on calendar aging of an open cathode fuel cell stack

Elodie Pahon, Samir Jemei, Jean-Pierre Chabriat, Daniel Hissel

Impact of the temperature on calendar aging of an open cathode fuel cell stack

E. Pahon[2], S. Jemei[1], J.-P. Chabriat[3], D. Hissel[1]

[1]FEMTO-ST Institute, FCLAB, Univ. Bourgogne Franche-Comté, CNRS, Belfort, France

[2] FEMTO-ST Institute, FCLAB, Univ. Bourgogne Franche-Comté, UTBM, CNRS, Belfort, France

[3]Energy-Lab (LE2P), Université de la Réunion, France

elodie.pahon@utbm.fr, samir.jemei@ubfc.fr, jean-pierre.chabriat@univ-reunion.fr,

daniel.hissel@ubfc.fr

Abstract: *This paper deals with calendar aging of a proton exchange membrane open-cathode fuel cell. Calendar aging is already developed for energy sources as supercapacitor and batteries but the literature is very poor for fuel cell stacks. However, this kind of test is necessary to determine the actual lifetime of the system without running it and to define the aging impact of the storage of such a system. One possible outcome for fuel cells is to provide electricity in remote areas without connection to the grid. This issue becomes even more challenging under hard environmental conditions, especially in areas with possible negative ambient temperatures. Experimental research on the degradation of open cathode fuel cells under these tricky conditions is needed to investigate the impact of resting states on the fuel cell lifetime and to evaluate the impact of the sub-zero temperatures on the performance losses.*

Keywords: *Proton exchange membrane open cathode fuel cell; calendar aging; accelerated stress tests; freeze-thaw cycles; negative temperature; performance losses.*

1. Introduction

The Proton Exchange Membrane Fuel Cell (PEMFC) is one of the most developed fuel cell technology in recent years [1]–[3]. It converts chemical energy in an electrical one at a low operating temperature

range from 60 to 80°C. The PEMFC is considered for a wide range of applications and power for both transport and stationary applications. Moreover, fuel cell technology seems to be a very promising solution to face the grid issues, especially on island or remote areas. In areas where the connection to the grid is impossible or difficult, the fuel cell coupled with renewable energies can fulfill the power (and/or heating) requirements to people. MYRTE project [4],[5] is one example of strong coupling between solar energy and hydrogen storage. The MYRTE platform is located in Corsica, France. Since 2012, 560 kW of solar panels are connected to a hydrogen-based storage system that provides a solution to the intermittency problem [6]–[8]. The electricity provided by solar panels array is transformed in hydrogen and oxygen thanks to an electrolyzer. Both gases produced are stored in high capacity tanks. When needed, oxygen and hydrogen can be re-used in a PEMFC to generate electricity for power grid supply. Contrary to island regions where the climate is warmer and wetter, another potential application of PEMFC in a remote area is in extreme climate regions including sub-freezing temperatures. For instance, HAEOLUS project used the energy of the wind to generate electricity and produce hydrogen by water electrolysis, above the Arctic Circle [9]. A new-generation electrolyzer is integrated within a state-of-the-art wind farm in North Norway with access to a weak power grid. Another example of remote areas are the high-altitude mountain refuges. A refuge in the Alps called “Refuge du Col du Palet” located at 2,600m above sea level is autonomous in energy as using solar panels, an electrolyzer and a fuel cell system. The hydrogen generated in winter (when the refuge is closed) is used in summer time for electricity production [10], [11]. The energy solution aims at seasonal balancing and long-term storage. In these extreme environmental conditions with negative temperature, it is well-known that the fuel cell is prone to freeze and thaw effects which leads to the formation of ice inside the stack. In the case of sub-zero temperatures, the water management inside the fuel cell stack is crucial [12]–[15]. The purge of the gas channels also plays a key role in the framework of cold temperatures to remove the water produced as well as possible [16], [17]. When freezing, the volume of water increases up to 9% of the initial volume (for liquid water) due to the difference between water and ice densities [18]. Chacko et al. [19] used the electrochemical

impedance spectra (EIS) and especially the high frequency resistance to observe the water hydration and estimate the ice formation during cold start operation. Mechanical damages could be observed due to the volume expansion as well as membrane [20], [21], gas diffusion layers (GDL) [21]–[24] and catalyst layers (CL) degradations [25], [26] with a loss of electrochemical active area and permanent damages [27], [28].

As for renewable energy systems, the most important requirement is the storage of energy without permanent losses and a long lifetime of the device, this paper investigates the durability of an open-cathode PEMFC while inactivity conditions. As mentioned above, depending on the area where the PEMFC is stored, the temperature (and humidity) change and impact the fuel cell performances, especially when considering open-cathode fuel cell stacks, where the electrolyte sites are in direct contact with ambient air. Many works deal with the influence of the temperature and humidity while the fuel cell is in operation [29]–[34]. However, the longtime storage under ambient or subfreezing temperatures is under-investigated.

Furthermore, in the case of an open-cathode fuel cell the negative temperature impact is higher than for closed-cathode fuel cell stacks for which the risks are limited because the stack is tight and the impacts are limited to side-effects. With an open-cathode fuel cell, the anode inlet is supplied with dry hydrogen and the cathode inlet is fed with air blowing coming from fans that are located in the front of the cells. The rotating movement of the blades allows the air to pass through the different cells in order to supply them with oxygen. The fan rotation speed also allows to regulate the operating temperature to a specific value. At the anode outlet, there is a purging valve for dead-ended operation and periodic purging [35]. The anode has to be purged regularly in order to flash out the accumulated water and built-up nitrogen. This is conducted by opening the anode outlet for a giving period that can vary depending on the current density or the water contents. Santangelo et al. [36] investigated the effects of load variation and purge cycles on an open-cathode fuel cell dedicated for stationary applications. Improper control of the purge can lead to hydrogen starvation along the channel due to

the accumulation of water and nitrogen in the anode, which not only decreased fuel cell performance but also triggered corrosion of the carbon as the catalyst support in the cathode [37]. Kurnia et al. [38] make a comprehensive review of researches on PEMFC operated in dead-end anode including: the performance losses due to hydrogen starvation, water accumulation and nitrogen crossover, and the mitigation strategies with purging strategy.

For these structural reasons, it is strongly important to investigate both the behavior of an open-cathode under long-time storage and under different temperatures to generalize the use of open-cathode fuel cells in remote area. In this paper, the use case that is studied concerns a high-mountain refuge. It is located at the “Col du Palet” in the French Alpes at an altitude of 2,600m. As an investigation, calendar aging tests are performed on two open-cathode fuel cells in order to observe the performance losses under ambient conditions (positive temperature and relative humidity both monitored) and under negative and subfreezing temperatures (up to -30°C). The literature on calendar aging tests on PEMFC is poor [39], unlike it is widely studied for batteries [40]–[47] and/or supercapacitors [48]–[54] since several years.

The aim of this work is to present the first experimental results of calendar aging tests of an open cathode PEMFC. First, the experimental setup is detailed as well as the test protocol and the characterization steps. The experimental results for both open cathode PEMFC calendar aging tests are presented in section 3 with the power losses, the study of reversible and irreversible degradations observed and the durability aspect considering the performance losses of the fuel cells. There is also a comparison of the performance losses between the two stacks stored under two different temperature conditions. Section 4 gives conclusions of the first calendar aging test on open-cathode PEMFC.

2. Experimental setup

2.1. Fuel cell stacks specifications and test bench

The open-cathode fuel cells used in this study are the commercial fuel cell stacks from Ballard company. Each fuel cell is composed of 13 cells for a power of 1kW. The basic operating specifications are detailed in Table 1 and Figure 1 presents a scheme of the test bench used to perform the characterizations needed to evaluate the performance degradation of both fuel cell stacks.

Table 1: Basic operating specifications of fuel cell stacks

<table>
<tr><th>Parameter</th><th colspan="8">Value / Range [unit]</th></tr>
<tr><td>Current</td><td colspan="8">0 – 75 [A]</td></tr>
<tr><td>Voltage</td><td colspan="8">0.5 – 1 [V/cell]</td></tr>
<tr><td>Stack temperature</td><td colspan="8"><table>
<tr><td>Stack current (A)</td><td>0</td><td>7.3</td><td>14.5</td><td>29.0</td><td>51.7</td><td>65.3</td><td>75.0</td></tr>
<tr><td>Maximum (°C)</td><td>52</td><td>55</td><td>57</td><td>62</td><td>70</td><td>75</td><td>75</td></tr>
<tr><td>Optimum (°C)</td><td>26</td><td>30</td><td>34</td><td>41</td><td>53</td><td>61</td><td>67</td></tr>
<tr><td>Minimum (°C)</td><td>6</td><td>10</td><td>14</td><td>21</td><td>33</td><td>41</td><td>47</td></tr>
</table></td></tr>
<tr><td>Start-up temperature</td><td colspan="8">Higher than -10°C</td></tr>
<tr><td>Gas inlet temperature
anode/cathode</td><td colspan="8">-15 to 65 [°C] / -20 to 52 [°C]</td></tr>
<tr><td>Inlet humidity
anode/cathode</td><td colspan="8">0 [%] / 0 – 100 [%]</td></tr>
<tr><td>Fuel pressure</td><td colspan="8">0.36 [barg]</td></tr>
<tr><td>Purge interval</td><td colspan="8">2300 [A.s]</td></tr>
</table>

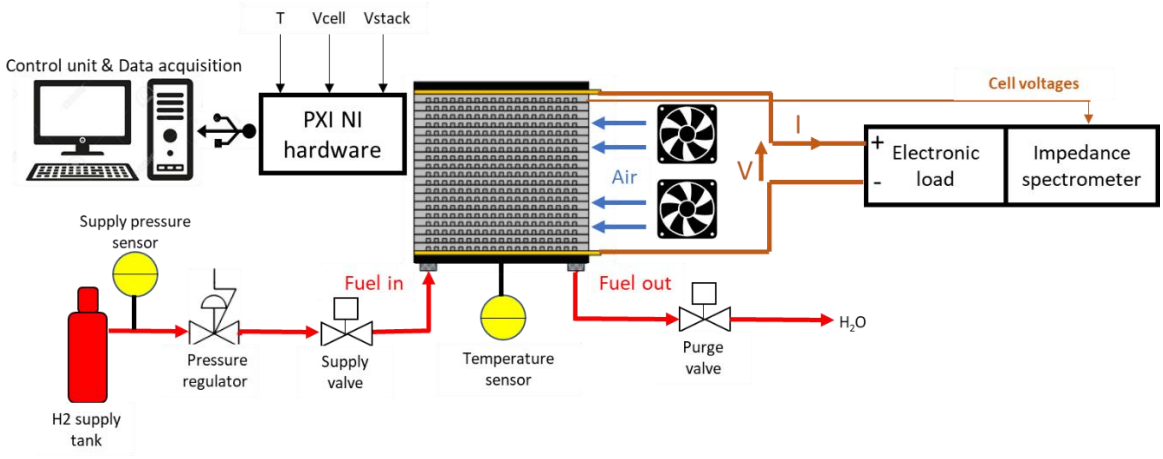

Figure 1: Scheme of the test bench

2.2. Experimental protocol

Two commercial self-humidified open-cathode fuel cell stacks are devoted to calendar ageing tests (FCgen® -1020ACS from Ballard). The first one is used as a reference meaning that it was stored inside a room where the temperature and the humidity are controlled (50% of humidity at 20°C). The stack stays in a resting state for two years, without any other special precaution. The second one is stored in a climate chamber under a sub-zero temperature. The temperature inside the chamber varies between -30°C and -2 °C in 24 hours. This freezing cycle is reproduced during three weeks. The temperature cycle used is an accelerated proposal of the actual temperature conditions in a mountain refuge. The cycle is accelerated approximatively 5 times, 3 weeks of sub-zero temperatures instead of 4 months of winter (from November to February). The temperature range is based on the actual meteorological observations from the refuge in winter, collected on National Centers for Environmental Information website.

Before cooling down the fuel cell stack, a purge of water and nitrogen contained at the anode outlet is made by operating several times the manual purge valve until there is no more visible water at the exhaust, in the transparent pipe. No nitrogen sweep is performed. Then, the fuel inlet and outlet are closed and the stack is placed inside the climate chamber. The temperature inside the climate chamber

decreased until reaching the given temperature of -30°C and then the freezing cycle can start. Obviously, the fuel cell stack did not run during the storage period inside the climate chamber. After 3 weeks' freezing cycles, the stack is left at room temperature during one day before restarting it. After this period, the ice that was formed inside the stack is estimated to have been melted. Then, the stack is heated by increasing progressively the current until it reaches the maximum current of 75A. The different steps and steady state conditions to achieve during the starting procedure are given in Table 2.

Table 2 : Heating procedure to restart the fuel cell stack

Step number	**Current [A]**	**Temperature [°C]**	**Resting time [min]**
Step 1	10	32	3
Step 2	20	37	3
Step 3	45	50	5
Step 4	60	57	5
Step 5	75	65	5

The performance of the stack was measured by varying the current from 75A (maximal current) to 0A and from 0A to 75A, in order to observe the voltage behavior and the hysteresis phenomenon. The operating conditions are the following: inlet fuel pressure is fixed at 0.36 barg, the stack temperature evolved with the current as mentioned in Tables 1 and 2 (maximum temperature = 75°C), the air relative humidity is fixed by the testing room at 50% at 20°C, the fuel relative humidity is not measured and the fuel cell is self-humidified, the flow rates are not measured as visible on the global scheme (cf. Figure 1). After performing the polarization curve, the stack is purged and stopped for a day before performing another polarization curve. A total of three polarization curves is obtained at a rate of one per day, in order to observe the possible performance recovery of the stack. After these three days, three EIS are performed by using an impedance spectrometer at three current levels: 15A, 45A and

70A. The EIS at a current of 15A is defined to observe mainly the activation losses at a low current value just before the beginning of the linear region of the polarization curve. A second EIS (at 45A) is performed as an intermediate current located in the linear region of the polarization curve. The last EIS is performed at 70A in order to observe the contribution of diffusion losses close to the maximal admissible current. The sweeping frequency ranged from 0.2Hz to 5000Hz with 10 points per decade and 3 periods at high frequencies (up to 10Hz) and 5 points per decade and 3 periods at low frequencies. The number of points per decade refers to the frequency division and thus to the number of frequency points considered to create the frequency vector. The number of periods refers to the number of points considered on the sinus perturbation. All of these parameters are defined based on the maximum purge interval value between two EIS at the maximal current value of 70A ($\frac{purge\ interval\ [A.s]}{Current\ [A]}$= 30 seconds) . It is a compromise between the purge interval, the desired number of frequency points and the precision of the EIS measurements while the fuel cell operates in nominal operating conditions (without performance degradation). The amplitude of the AC signal is $\pm$10% of the DC current except for the last EIS at 70A, because of the current limitation of 75A. In this case, the amplitude of the AC signal is $\pm$5%. When all the characterizations are performed, the stack is unplugged from the test bench, the fuel inlet and outlet are closed and the stack is cooled down a new time. Figure 2 shows this experimental procedure.

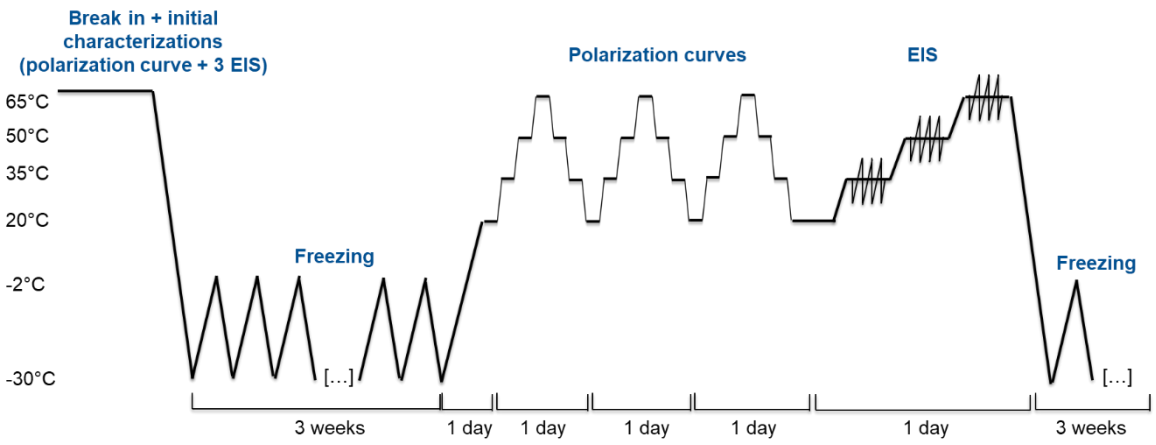

Figure 2: Procedure of the calendar ageing experiment

3. Results and discussion

3.1. Performance degradation with freezing cycles

Figure 3 shows the evolution of the performance degradation, after 2 years of accelerated freeze-thaw cycles, representing approx. 10 years of winter storage. The polarization curves are measured just after the freezing period inside the climate chamber. Thus, both the reversible and irreversible losses are merged in the voltage degradation.

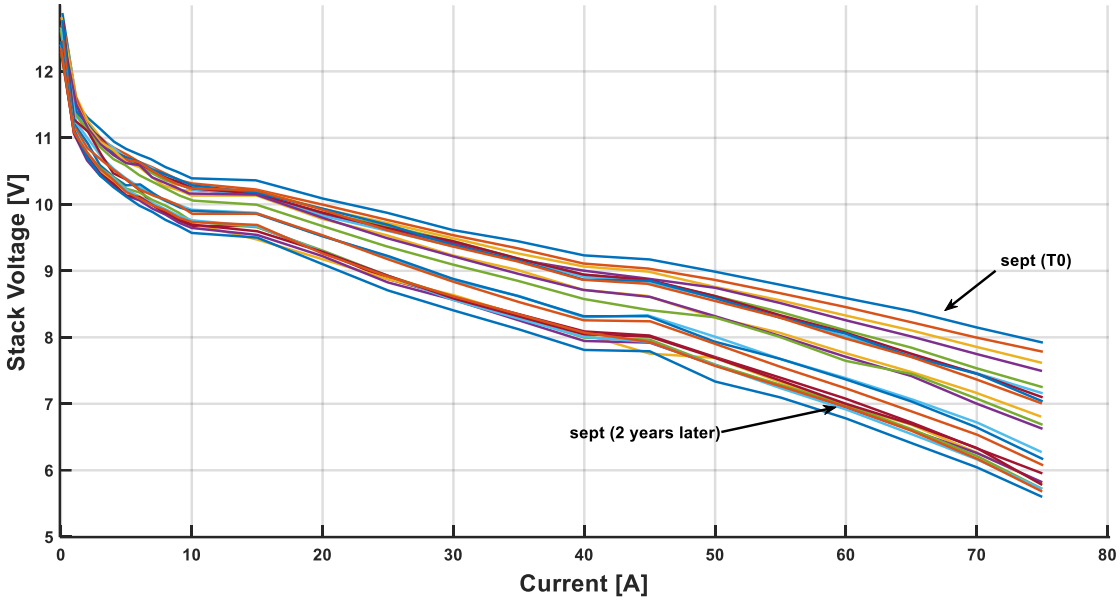

Figure 3: Polarization curves over calendar aging

Performance degradation was observed as the freeze-thaw cycles progressed. In order to better see the voltage degradation, Figure 4 presented the voltage behavior of the PEMFC with the number of freezing cycles at currents set to 0, 15, 45 and 75A. At Open Circuit Voltage (OCV) (0 Amp), the voltage level is quite constant even if there are some fluctuations due to the reversible losses and performance recovery between two freezing cycles. When the fuel cell stack is cooled down below the freezing temperature, the liquid water blocked inside the stack forms ice. That leads to mechanical damages due to volume expansion during freezing or from frost heave [55]. Some cracks or pinholes could appear on the membrane that leads to hydrogen crossover. Hydrogen crossover from the anode to

cathode can affect the decrease in OCV of the fuel cells [22], [56]. The catalyst layer is also delaminated leading to a proton and electron conductivity drop [57]. Finally, ice formation damaged the surface, the porosity and the tortuosity of the GDL that causes a loss of the active area [24], [58].

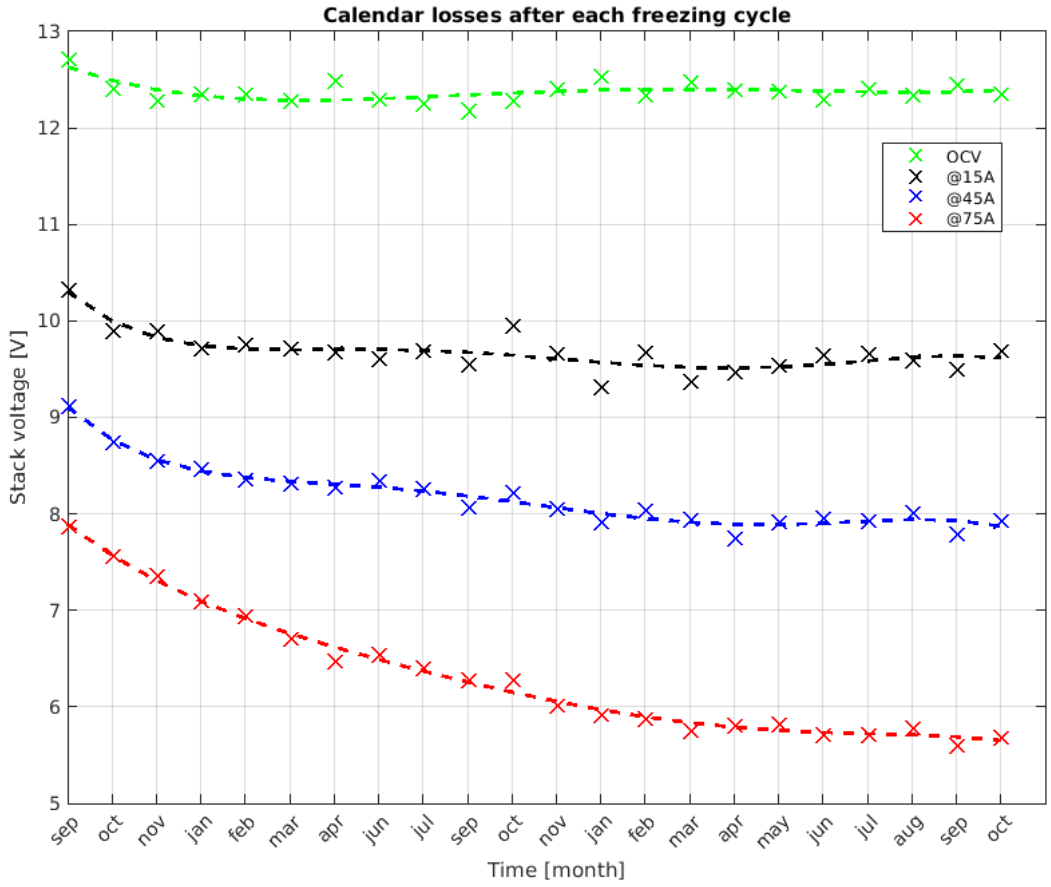

Figure 4: Effects of the calendar aging on the performance of the open-cathode fuel cell

In our case, the membrane does not seem to be so damaged by repetitive freezing cycles. However, the voltage degradation is strengthened as the current increased. This can be due to an increasing of the charge transfer resistance and mass transfer resistance associated to freezing cycles. A first rapid slope of degradation is clearly visible from the beginning of the test to April (7 months later). Then, there is another slope from April to September (on the same year), with a performance recovery in June. This could be explained by the missing characterization in May. Sometimes, some characterizations are missing as they are scheduled during the holidays or owing to unavoidable experimental problem. For the month where no characterization is done, the stack is stored at the

ambient room instead of inside the climate chamber and sub-zero temperatures. Thus, an increase of the resting time at ambient temperature may produce a recovery of the catalyst sites. During the time period of storage in ambient conditions, the temperature of the stack increased and the ice melts. The water trapped inside the fuel cell is not evacuated from it, but as the ionomer is very hydrophilic, the water may migrate and hydrate the membrane besides the back-diffusion effect (from the cathode to the anode side) with the gradient of the water concentration [59][60]. In addition, it was observed during the experiments that the fuel cell was more difficult to restart when it had remained stored for a long time at room temperature and that it had to be purged much more regularly to be able to restart it. It could be due to flooding as it has been observed that water flooding in PEMFCs is gravity dependent [61].

During the last year, from October to October, the trend of degradation could be represented by a linear regression. It is noticeable that the permanent damages on the catalyst layer such as loss of active area occurs at the first freezing cycles and then the degradation gradient is slower. To conclude, the accumulation of irreversible losses under repetitive freezing causes permanent degradation of the open-cathode PEMFC.

Figure 5 presents the EIS spectra with the freezing cycles effects for 3 current levels: 15, 45 and 70A and for three different time periods: at the beginning of the test in September, one year later and two years later.

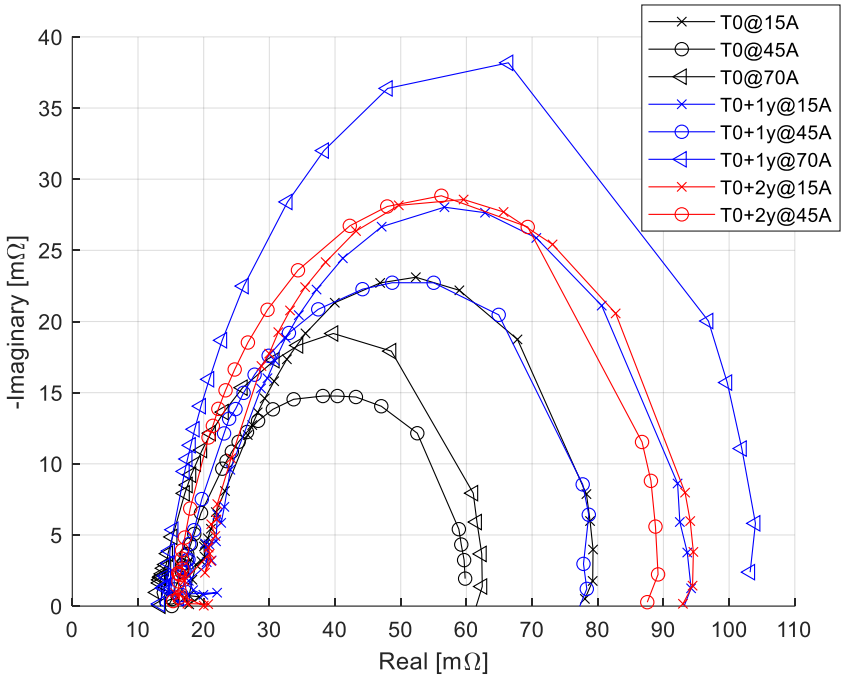

Figure 5: EIS plots according to calendar aging and current density

As the current increases, the semicircle first decreases in size and subsequently it increases. The semicircle size decrease is ascribed to an electrochemical process (oxygen reduction) with a kinetic resistance that is inversely proportional to the current (Tafel behavior). In contrast, the semicircle size increase is attributed to oxygen mass transfer. The ohmic resistance *Rm* increases more for the high current densities. Lots of variations of *Rm* are observed under low current densities, thus supporting the view that the membrane is more affected under low currents. At low current density, the polarization resistance *Rp* at *T0+1 year* is similar to those one year later that might mean the degradation is no longer changing so much. By comparing with Figure 4, the voltage value at September (first year) and September (second year) are very close, depending on the current level. For EIS at 45 and 70A, the polarization resistance increases hugely with calendar aging. Therefore, it is even no longer possible to plot the EIS at 70A without reaching the maximum stack temperature. This phenomenon might be explained by the mass transport losses effects resulting from high current levels. In addition, the concurrent increase in kinetic and mass transport losses could equally be due to the presence of contaminant [62], [63]. Contaminants can easily adsorb on the catalyst surface

because the cathode is exposed to ambient air for long periods of time at a cell potential that would be insufficient (~0 V cell voltage) to oxidize or reduce many species. But, the presence of contaminants could be ascertained with air sample analyses and additional diagnostics such as cyclic voltammetry to identify the presence of foreign species on the catalyst surface. Another observation is that the *Rp* value at 15A at *T0* is the same as the one obtained at 45A at *T0+1 year*.

Table 3 details the resistance variation over time and current density, with *Rm* the total ohmic resistance for all components of the fuel cell (crossing the real axis at high frequency) and *Rp* is the total polarization resistance (crossing the real axis at low frequency) including activation and mass transport resistance. As accelerated tests are performed for freeze-thaw cycles, a corresponding real time duration is also mentioned in Table 3. As a reminder, each cycle of 3 weeks can be considered to be roughly 4 real months (thus an accelerated ratio of about 5 according to our experimental protocol). So, the actual 2 years of testing would correspond to the actual 10 years of storage in winter.

Table 3: Ohmic and polarization resistance values over time and current density

Curve	Black cross	Black circle	Black triangle	Blue cross	Blue circle	Blue triangle	Red cross	Red circle
Current level [A]	15	45	70	15	45	70	15	45
Testing time with accelerated freeze-thaw cycles [year]	0	0	0	1	1	1	2	2
Number of freeze-thaw cycles	0	0	0	10	10	10	21	21
Corresponding real time duration [year]	0	0	0	5	5	5	10	10
Rm [mΩ]	17.60	14	12.45	17.52	16.29	13.98	18.62	15.35
Rp [mΩ]	78	60	61	92	77	103	92	87.5

3.2. Recoverable performance

In this work, the recovery operation is performed additionally: several polarization curves are done, one per day, until the two last performed polarization curves are quite similar. The number of repetitions was determined at the beginning of the test. For the first characterization period, only two polarization curves are done after which the voltage value is stabilized. Four polarization curves are performed at the second characterization time where it appears that the fourth and the third polarization curves are quite similar considering the voltage value. Thus, the value of three successive polarization curves appears as a good compromise for studying the reversible losses. Figure 6 shows the performance recoveries at 0A (OCV), 15A, 45A and 75A.

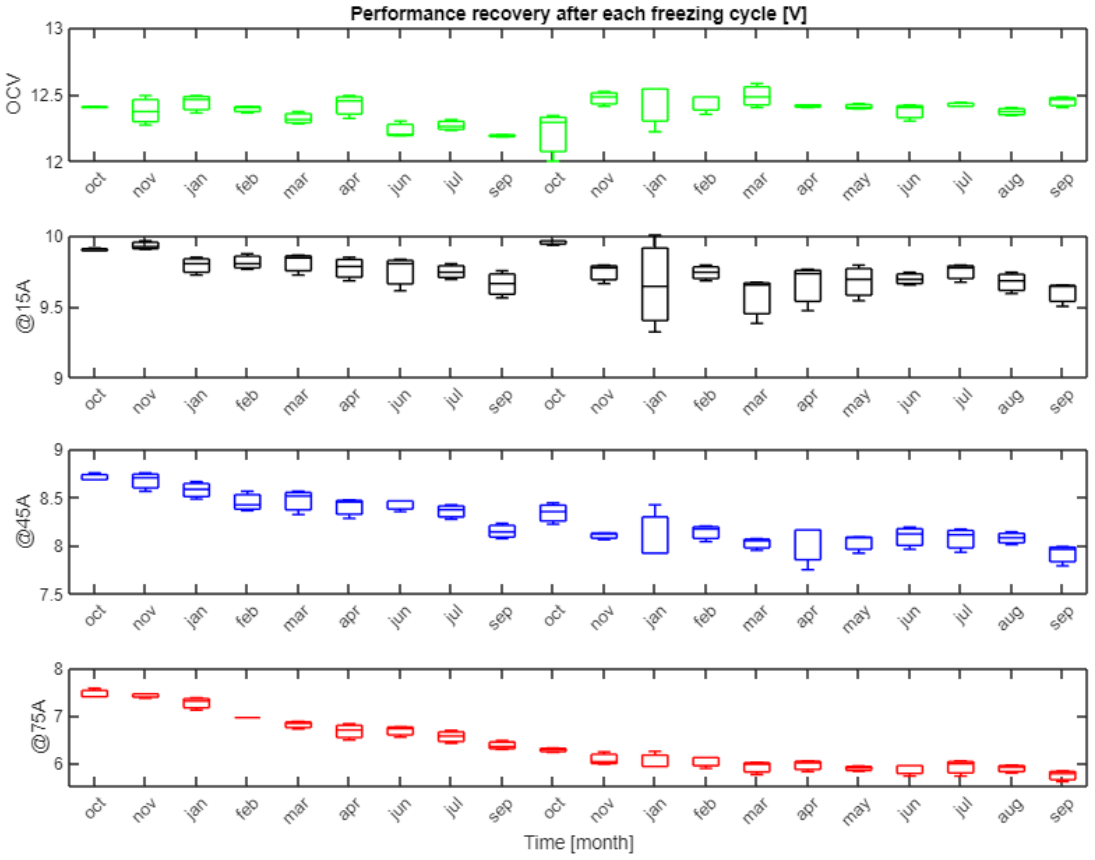

Figure 6: Evolution of the performance recovery with freezing cycles in Volts for 4 current levels

At OCV, the recovery may be considered as negligible. For other current levels, a voltage recovery is noticeable even if the recovery amplitude (about 0.2V) is quite similar with the freezing cycles. After each missing characterization, the largest recovery is observed (amplitude of the box plots).

After a month exposure to ambient temperature, the catalyst area regenerated. At OCV, there is no recovery but rather a loss of performance between the two latest polarization curves. This phenomenon is probably due to hydrogen crossover, that is one of the two major factors causing a reduction of fuel cell OCVs [56], [64]. The month following a significant voltage recovery (February), the recovery is poor at each current level meaning that only irreversible degradations are visible. The last observation is about the amount of the reversible losses. The higher the number of freezing cycles, the lower the recovery between the two last polarization curves (from 0.1V in the first year to 0.04V in the second year). For instance, in August (second year), the three polarization curves are merged.

The durability remains an issue for fuel cell systems in case of running operation as well as during long period of inactivity because of the performance losses. The aim of this paper is to investigate the durability of an open-cathode PEMFC under calendar aging for a stationary application which is a high mountain refuge. The Department of Energy (DoE) in United-States defined the end-of-life of such a fuel cell system as a loss of 20% of the initial nominal power (541W for fuel cell #1) [65]. Figure 7 presents the power losses over time in month, at nominal value (65A). The 20% of the nominal power losses is reached after 2 years of freezing cycles while a high degradation is observed during the first four months of lifetime.

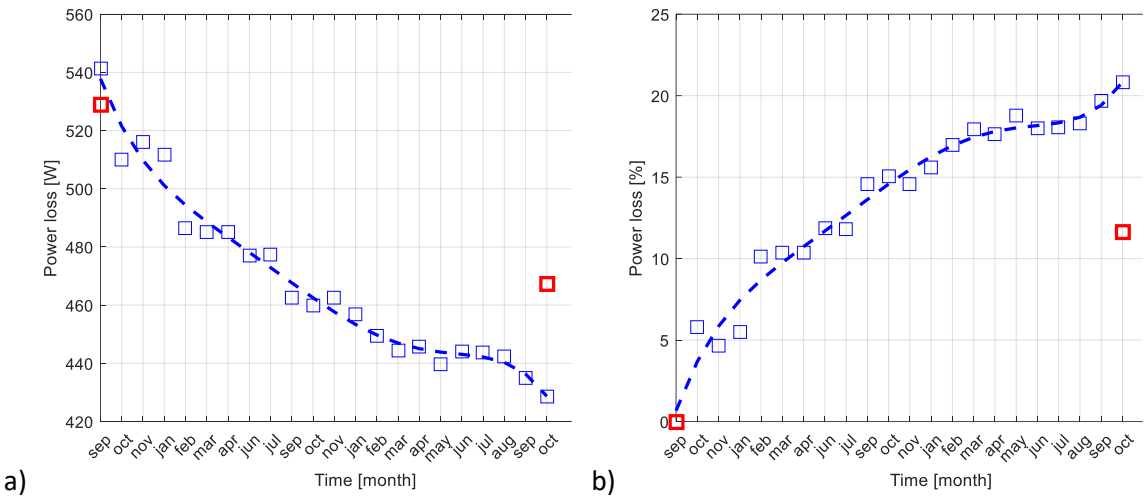

Figure 7: Power losses (red squares for FC#1 and blue squares for FC#2) over time a) in Watt losses b) in percentage of losses

Finally, a comparison between the two fuel cell stacks has to be done in order to observe the impact of the temperature on the degradation while open-cathode fuel cells calendar aging. As a reminder, the first fuel cell stack is stored in a room with a controlled temperature and humidity (50% RH at 20°C) and the second fuel cell stack is stored during 3 weeks under sub-zero temperatures. The initial nominal power of fuel cell #1 was 529W (12W less than fuel cell #2). After two years of inactivity, the nominal power is 467W that gives a loss of 62W yielding to a power loss of 12%. The degradation considers the same performance recovery protocol namely 3 successive polarization curves.

Figure 8 presents the polarizations curves performed at the beginning of the test on September and two years later for both open-cathode fuel cells. For both fuel cells the activation losses and diffusion losses increased over time and the ohmic losses also growing for fuel cell #2 which was exposed to severe negative temperature.

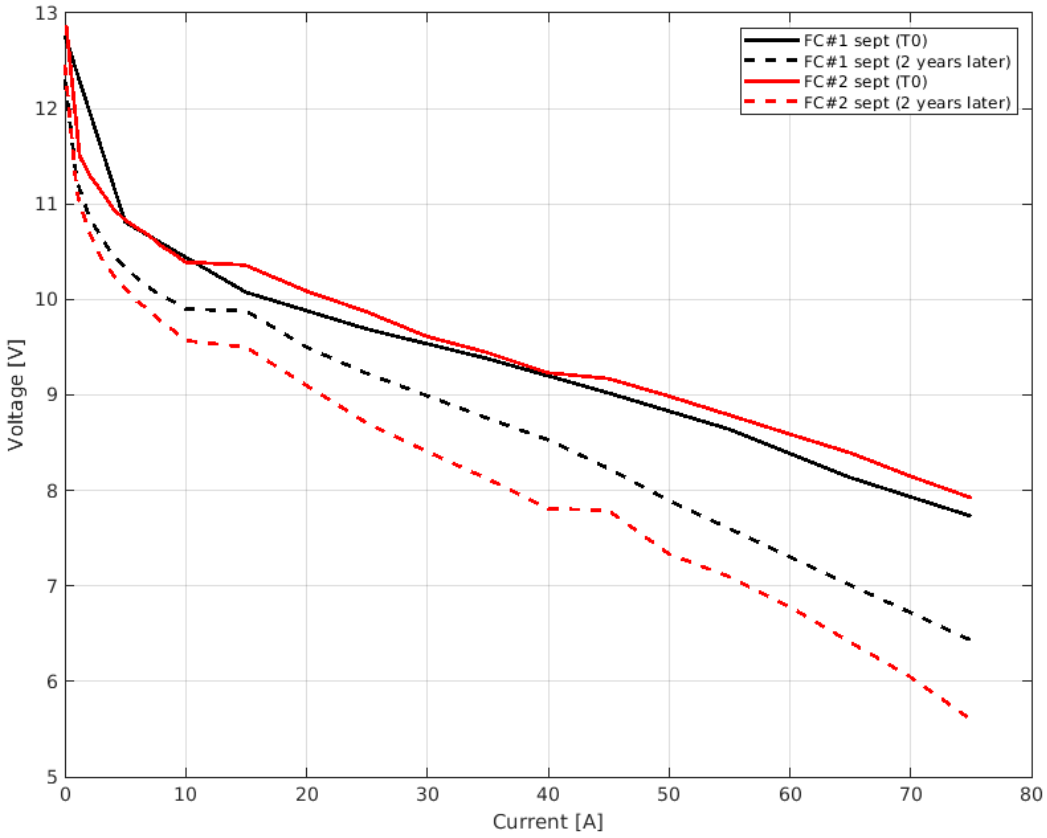

Figure 7: Polarization curves performed at the beginning of the calendar aging (solid lines) and two years later (dashed lines) for both open-cathode fuel cells where FC#1 (black lines) is stored under ambient temperature and hygrometry conditions and FC#2 (red lines) is stored under sub-zero temperatures

4. Conclusion

As proton exchange membrane fuel cells appear as a promising technology to produce heat and electricity in remote areas, the durability aspects need to be studied. The lifetime of the fuel cell system has to be investigated under actual operating conditions as well as under long-time storage and inactivity periods. As for renewable energy systems, the most important requirement is the storage of energy without permanent losses by self-discharge and a long lifetime, calendar aging tests has to be performed with fuel cells as it has been done for years for batteries or supercapacitors. Here, calendar aging tests were performed on open-cathode fuel cells as they are: i) suitable for stationary applications in remote area without connection to the grid, ii) obviously more prone to environmental varying conditions than closed-cathode fuel cells. Additionally, the impact of the temperature is

investigated as the remote areas considered could be extreme cold areas as in high mountain refuge. Considering this kind of stationary applications, the open cathode fuel cell is obviously exposed to negative temperature during a large part of the year. The results of the calendar aging tests performed on open-cathode fuel cells show that the degradation is lower under ambient temperature conditions than under sub-zero temperature where water freezing is unavoidable. The impact of ice formation under negative temperature is largely visible at high current densities owing to a loss of mass transport and charge transfer. The membrane does not appear to have undergone severe degradation as the performance losses at OCV are quite constant over time. The performance recovery is also studied in this paper and the recovery ratio decreased over time, which means that the irreversible damages on the fuel cell stack are less and less recoverable over time. A possible way to let the fuel cell components (i.e. catalyst layer) regenerate is to put the stack under ambient conditions for several days. However, flooding effect are more significant when wanting to restart the fuel cell system in this case. After two years of storage, the open-cathode fuel cell exposed to negative temperature cycles (FC#2) lost 20% of its initial nominal power against 12% for the other open-cathode fuel cell stored under ambient conditions (FC#1). A long-time storage clearly impacts the performance of both open-cathode PEMFC whether at ambient or negative temperatures. Nevertheless, the stack FC#2 achieved the end-of-life threshold defined by the US DOE, unlike the other one (FC#1). The results obtained on the stack FC#2 can be attributed to a change in storage temperature but also to a different cumulative stack operation duration. As future works, additional experiments will be needed to separate temperature and operation contributions. For instance, another calendar aging test must be performed under ambient temperature conditions with a characterization every month to evaluate the degradation linked to the cumulative running operations.

5. Acknowledgment

The authors would like to thank the Bourgogne Franche-Comte region, for financially supporting this work and offering the possibility to use their data. This work has been supported by the EIPHI Graduate

School (contract ANR-17-EURE-0002) and the Region Bourgogne Franche-Comté and the French National H2 & Fuel Cell Network (FRH2 CNRS).

References

[1] T. Özgür and A. C. Yakaryılmaz, "A review: Exergy analysis of PEM and PEM fuel cell based CHP systems," *Int. J. Hydrogen Energy*, vol. 43, no. 38, pp. 17993–18000, 2018.

[2] Y. Wang, D. F. Ruiz Diaz, K. S. Chen, Z. Wang, and X. C. Adroher, "Materials, technological status, and fundamentals of PEM fuel cells – A review," *Mater. Today*, vol. 32, pp. 178–203, 2020.

[3] O. Z. Sharaf and M. F. Orhan, "An overview of fuel cell technology: Fundamentals and applications," *Renew. Sustain. Energy Rev.*, vol. 32, pp. 810–853, Apr. 2014.

[4] P. Poggi, C. Darras, M. Muselli, and G. Pigelet, "The PV-Hydrogen MYRTE Platform - PV Output Power Fluctuations Smoothing," *Energy Procedia*, vol. 57, pp. 607–616, 2014.

[5] C. Darras, M. Muselli, P. Poggi, C. Voyant, J.-C. Hoguet, and F. Montignac, "PV output power fluctuations smoothing: The MYRTE platform experience," *Int. J. Hydrogen Energy*, vol. 37, no. 19, pp. 14015–14025, 2012.

[6] "MYRTE hydrogen energy storage test powers up in Corsica," *Fuel Cells Bull.*, vol. 2014, no. 6, p. 8, 2014.

[7] P. Moriarty and D. Honnery, "Intermittent renewable energy: The only future source of hydrogen?," *Int. J. Hydrogen Energy*, vol. 32, no. 12, pp. 1616–1624, 2007.

[8] J. Michalski, "Investment decisions in imperfect power markets with hydrogen storage and large share of intermittent electricity," *Int. J. Hydrogen Energy*, vol. 42, no. 19, pp. 13368–13381, 2017.

[9] "HAEOLUS project website." [Online]. Available: www.haeolus.eu.

[10] D. Morin, Y. Stevenin, and P. Brault, “Energy Management of isolated DC microgrids with hybrid batteries-hydrogen storage system using Model Predictive Control and Wavelet Neural Networks based forecasts,” in *2019 21st European Conference on Power Electronics and Applications (EPE ’19 ECCE Europe)*, 2019, p. P.1-P.10.

[11] “Hydrogen power for French alpine refuge,” *Fuel Cells Bull.*, vol. 2015, no. 7, p. 6, 2015.

[12] A. O. Pistono and C. A. Rice, “Subzero water distribution in proton exchange membrane fuel cells: Effects of preconditioning method,” *Int. J. Hydrogen Energy*, vol. 44, no. 39, pp. 22098–22109, 2019.

[13] M. Zhu, X. Xie, K. Wu, A.-U.-H. Najmi, and K. Jiao, “Experimental investigation of the effect of membrane water content on PEM fuel cell cold start,” *Energy Procedia*, vol. 158, pp. 1724–1729, 2019.

[14] L. Yao, J. Peng, J. Zhang, and Y. Zhang, “Numerical investigation of cold-start behavior of polymer electrolyte fuel cells in the presence of super-cooled water,” *Int. J. Hydrogen Energy*, vol. 43, no. 32, pp. 15505–15520, 2018.

[15] Y. Ishikawa, T. Morita, K. Nakata, K. Yoshida, and M. Shiozawa, “Behavior of water below the freezing point in PEFCs,” *J. Power Sources*, vol. 163, no. 2, pp. 708–712, 2007.

[16] S. Strahl, A. Husar, and J. Riera, “Experimental study of hydrogen purge effects on performance and efficiency of an open-cathode Proton Exchange Membrane fuel cell system,” *J. Power Sources*, vol. 248, pp. 474–482, 2014.

[17] J. Hou *et al.*, “Analysis of PEMFC freeze degradation at −20°C after gas purging,” *J. Power Sources*, vol. 162, no. 1, pp. 513–520, 2006.

[18] A. A. Amamou, S. Kelouwani, L. Boulon, and K. Agbossou, “A Comprehensive Review of Solutions and Strategies for Cold Start of Automotive Proton Exchange Membrane Fuel Cells,” *IEEE Access*, vol. 4, pp. 4989–5002, 2016.

[19] C. Chacko, R. Ramasamy, S. Kim, M. Khandelwal, and M. Mench, “Characteristic Behavior of Polymer Electrolyte Fuel Cell Resistance during Cold Start,” *J. Electrochem. Soc.*, vol. 155, no. 11, p. B1145, 2008.

[20] Y. Tabe, M. Saito, K. Fukui, and T. Chikahisa, “Cold start characteristics and freezing mechanism dependence on start-up temperature in a polymer electrolyte membrane fuel cell,” *J. Power Sources*, vol. 208, pp. 366–373, 2012.

[21] S. Kim, B. K. Ahn, and M. M. Mench, “Physical degradation of membrane electrode assemblies undergoing freeze/thaw cycling: Diffusion media effects,” *J. Power Sources*, vol. 179, no. 1, pp. 140–146, 2008.

[22] K. D. Baik, S. Il Kim, B. K. Hong, K. Han, and M. S. Kim, “Effects of gas diffusion layer structure on the open circuit voltage and hydrogen crossover of polymer electrolyte membrane fuel cells,” *Int. J. Hydrogen Energy*, vol. 36, no. 16, pp. 9916–9925, 2011.

[23] C. Lee and W. Mérida, “Gas diffusion layer durability under steady-state and freezing conditions,” *J. Power Sources*, vol. 164, no. 1, pp. 141–153, 2007.

[24] Y. Lee, B. Kim, Y. Kim, and X. Li, “Effects of a microporous layer on the performance degradation of proton exchange membrane fuel cells through repetitive freezing,” *J. Power Sources*, vol. 196, no. 4, pp. 1940–1947, Feb. 2011.

[25] R. Alink, D. Gerteisen, and M. Oszcipok, “Degradation effects in polymer electrolyte membrane fuel cell stacks by sub-zero operation—An in situ and ex situ analysis,” *J. Power Sources*, vol. 182, no. 1, pp. 175–187, 2008.

[26] Z. Zhan, H. Zhao, P. C. Sui, P. Jiang, M. Pan, and N. Djilali, “Numerical analysis of ice-induced stresses in the membrane electrode assembly of a PEM fuel cell under sub-freezing operating conditions,” *Int. J. Hydrogen Energy*, vol. 43, no. 9, pp. 4563–4582, 2018.

[27] J. P. Sabawa and A. S. Bandarenka, “Degradation mechanisms in polymer electrolyte

membrane fuel cells caused by freeze-cycles: Investigation using electrochemical impedance spectroscopy," *Electrochim. Acta*, vol. 311, pp. 21–29, 2019.

[28] J. Mishler, Y. Wang, P. P. Mukherjee, R. Mukundan, and R. L. Borup, "Subfreezing operation of polymer electrolyte fuel cells: Ice formation and cell performance loss," *Electrochim. Acta*, vol. 65, pp. 127–133, 2012.

[29] B. Zhang, F. Lin, C. Zhang, R. Liao, and Y.-X. Wang, "Design and implementation of model predictive control for an open-cathode fuel cell thermal management system," *Renew. Energy*, vol. 154, pp. 1014–1024, 2020.

[30] Q. Jian, B. Huang, L. Luo, J. Zhao, S. Cao, and Z. Huang, "Experimental investigation of the thermal response of open-cathode proton exchange membrane fuel cell stack," *Int. J. Hydrogen Energy*, vol. 43, no. 29, pp. 13489–13500, 2018.

[31] L. Vichard, R. Petrone, F. Harel, A. Ravey, P. Venet, and D. Hissel, "Long term durability test of open-cathode fuel cell system under actual operating conditions," *Energy Convers. Manag.*, vol. 212, p. 112813, 2020.

[32] H. Al-Zeyoudi, A. P. Sasmito, and T. Shamim, "Performance evaluation of an open-cathode PEM fuel cell stack under ambient conditions: Case study of United Arab Emirates," *Energy Convers. Manag.*, vol. 105, pp. 798–809, 2015.

[33] K. Ou, W.-W. Yuan, M. Choi, S. Yang, and Y.-B. Kim, "Performance increase for an open-cathode PEM fuel cell with humidity and temperature control," *Int. J. Hydrogen Energy*, vol. 42, no. 50, pp. 29852–29862, 2017.

[34] C. Mahjoubi, J.-C. Olivier, S. Skander-mustapha, M. Machmoum, and I. Slama-belkhodja, "An improved thermal control of open cathode proton exchange membrane fuel cell," *Int. J. Hydrogen Energy*, vol. 44, no. 22, pp. 11332–11345, 2019.

[35] S. Strahl, N. Gasamans, J. Llorca, and A. Husar, "Experimental analysis of a degraded open-

cathode PEM fuel cell stack," *Int. J. Hydrogen Energy*, vol. 39, no. 10, pp. 5378–5387, Mar. 2014.

[36] P. T. Paolo E. Santangelo, "Effects of load variation and purge cycles on the efficiency of Polymer Electrolyte Membrane Fuel Cells for stationary applications," *J. Renew. Sustain. Energy*, vol. 10, no. 014301, 2018.

[37] S. Strahl, A. Husar, and J. Riera, "Experimental study of hydrogen purge effects on performance and efficiency of an open-cathode Proton Exchange Membrane fuel cell system," *J. Power Sources*, vol. 248, pp. 474–482, Feb. 2014.

[38] J. C. Kurnia, A. P. Sasmito, and T. Shamim, "Advances in proton exchange membrane fuel cell with dead-end anode operation: A review," *Appl. Energy*, 2019.

[39] Y. Fang *et al.*, "Experimental investigation of performance degradation on an open cathode Proton Exchange Membrane Fuel Cell stored at sub-zero temperatures," in *International Conference on "Fundamentals & Development of Fuel Cells FDFC2017*, 2017.

[40] B. Balagopal, C. S. Huang, and M. Y. Chow, "Effect of calendar aging on li ion battery degradation and SOH," *Proc. IECON 2017 - 43rd Annu. Conf. IEEE Ind. Electron. Soc.*, vol. 2017-Janua, pp. 7647–7652, 2017.

[41] S. Grolleau *et al.*, "Calendar aging of commercial graphite/LiFePO4 cell – Predicting capacity fade under time dependent storage conditions," *J. Power Sources*, vol. 255, pp. 450–458, Jun. 2014.

[42] B. Stiaszny, J. C. Ziegler, E. E. Krauß, M. Zhang, J. P. Schmidt, and E. Ivers-Tiffée, "Electrochemical characterization and post-mortem analysis of aged LiMn2O4–NMC/graphite lithium ion batteries part II: Calendar aging," *J. Power Sources*, vol. 258, pp. 61–75, Jul. 2014.

[43] E. Redondo-Iglesias, P. Venet, and S. Pelissier, "Calendar and cycling ageing combination of batteries in electric vehicles," *Microelectron. Reliab.*, vol. 88–90, pp. 1212–1215, Sep. 2018.

[44] E. Redondo-Iglesias, P. Venet, and S. Pelissier, “Eyring acceleration model for predicting calendar ageing of lithium-ion batteries,” *J. Energy Storage*, vol. 13, pp. 176–183, Oct. 2017.

[45] J. Schmitt, A. Maheshwari, M. Heck, S. Lux, and M. Vetter, “Impedance change and capacity fade of lithium nickel manganese cobalt oxide-based batteries during calendar aging,” *J. Power Sources*, vol. 353, pp. 183–194, Jun. 2017.

[46] S. L. Hahn, M. Storch, R. Swaminathan, B. Obry, J. Bandlow, and K. P. Birke, “Quantitative validation of calendar aging models for lithium-ion batteries,” *J. Power Sources*, vol. 400, pp. 402–414, Oct. 2018.

[47] M. Dubarry, N. Qin, and P. Brooker, “Calendar aging of commercial Li-ion cells of different chemistries – A review,” *Curr. Opin. Electrochem.*, vol. 9, pp. 106–113, Jun. 2018.

[48] H. El Brouji, O. Briat, J.-M. Vinassa, N. Bertrand, and E. Woirgard, “Comparison between changes of ultracapacitors model parameters during calendar life and power cycling ageing tests,” *Microelectron. Reliab.*, vol. 48, no. 8–9, pp. 1473–1478, Aug. 2008.

[49] H. Gualous, R. Gallay, M. Al Sakka, A. Oukaour, B. Tala-Ighil, and B. Boudart, “Calendar and cycling ageing of activated carbon supercapacitor for automotive application,” *Microelectron. Reliab.*, vol. 52, no. 9–10, pp. 2477–2481, Sep. 2012.

[50] H. El Brouji, O. Briat, J.-M. Vinassa, H. Henry, and E. Woirgard, “Analysis of the dynamic behavior changes of supercapacitors during calendar life test under several voltages and temperatures conditions,” *Microelectron. Reliab.*, vol. 49, no. 9–11, pp. 1391–1397, Sep. 2009.

[51] A. Oukaour, B. Tala-Ighil, M. AlSakka, H. Gualous, R. Gallay, and B. Boudart, “Calendar ageing and health diagnosis of supercapacitor,” *Electr. Power Syst. Res.*, vol. 95, pp. 330–338, Feb. 2013.

[52] A. Oukaour, B. Tala-Ighil, M. AlSakka, H. Gualous, R. Gallay, and B. Boudart, “Calendar ageing and health diagnosis of supercapacitor,” *Electr. Power Syst. Res.*, vol. 95, pp. 330–338, Feb.

2013.

[53] O. Briat, J.-M. Vinassa, N. Bertrand, H. El Brouji, J.-Y. Delétage, and E. Woirgard, “Contribution of calendar ageing modes in the performances degradation of supercapacitors during power cycling,” *Microelectron. Reliab.*, vol. 50, no. 9–11, pp. 1796–1803, Sep. 2010.

[54] M. Ayadi, O. Briat, A. Eddahech, R. German, G. Coquery, and J. M. Vinassa, “Thermal cycling impacts on supercapacitor performances during calendar ageing,” *Microelectron. Reliab.*, vol. 53, no. 9–11, pp. 1628–1631, Sep. 2013.

[55] S. Palecki, S. Gorelkov, J. Wartmann, and A. Heinzel, “Frost induced damages within porous materials - from concrete technology to fuel cells technique,” *J. Power Sources*, vol. 372, pp. 204–211, 2017.

[56] A. A. Kulikovsky, “Hydrogen crossover impedance of a PEM fuel cell at open circuit,” *Electrochim. Acta*, vol. 247, pp. 730–735, 2017.

[57] A. Tavassoli *et al.*, “Effect of catalyst layer defects on local membrane degradation in polymer electrolyte fuel cells,” *J. Power Sources*, vol. 322, pp. 17–25, 2016.

[58] L. R. Jordan, A. K. Shukla, T. Behrsing, N. R. Avery, B. C. Muddle, and M. Forsyth, “Diffusion layer parameters influencing optimal fuel cell performance,” *J. Power Sources*, vol. 86, no. 1, pp. 250–254, 2000.

[59] D. Cha, W. Yang, and Y. Kim, “Performance improvement of self-humidifying PEM fuel cells using water injection at various start-up conditions,” *Energy*, vol. 183, pp. 514–524, 2019.

[60] Q. Jian, L. Luo, B. Huang, J. Zhao, S. Cao, and Z. Huang, “Experimental study on the purge process of a proton exchange membrane fuel cell stack with a dead-end anode,” *Appl. Therm. Eng.*, vol. 142, pp. 203–214, Sep. 2018.

[61] H. Guo, X. Liu, J. F. Zhao, F. Ye, and C. F. Ma, “Effect of low gravity on water removal inside

proton exchange membrane fuel cells (PEMFCs) with different flow channel configurations," *Energy*, vol. 112, pp. 926–934, 2016.

[62] J. Qi, Y. Zhai, and J. St-Pierre, "Effect of contaminant mixtures in air on proton exchange membrane fuel cell performance," *J. Power Sources*, vol. 413, pp. 86–97, Feb. 2019.

[63] B. Shabani, M. Hafttananian, S. Khamani, A. Ramiar, and A. A. Ranjbar, "Poisoning of proton exchange membrane fuel cells by contaminants and impurities: Review of mechanisms, effects, and mitigation strategies," *J. Power Sources*, vol. 427, pp. 21–48, Jul. 2019.

[64] J. Zhang, Y. Tang, C. Song, J. Zhang, and H. Wang, "PEM fuel cell open circuit voltage (OCV) in the temperature range of 23°C to 120°C," *J. Power Sources*, vol. 163, no. 1, pp. 532–537, 2006.

[65] DOE, "DOE Technical Targets for Fuel Cell Systems for Stationary (Combined Heat and Power) Applications," 2015.